ON THE FEASIBILITY OF MICROWAVE PRODUCED BRAGG REFLECTOR: EXAMINED BY THE CHAMBER EXPERIMENT

S. P. Kuo and Y. S. Zhang
Weber Research Institute, Polytechnic University,
Route 110, Farmingdale, NY 11735, U. S. A.

Paul Kossey
Air Force Geophysics Laboratory
Hanscom AFB, MA 01731, U. S. A.

Robert J. Barker
Air Force Office of Scientific Research
Bolling AFB DC 20332-6448 U. S. A.

ABSTRACT

A set of parallel plasma layers is generated by two intersecting microwave pulses in a chamber containing dry air at a pressure comparable to the upper atmosphere. The dependencies of breakdown conditions on the pressure and pulse length are examined. The results are shown to be consistent with the appearance of tail erosion of microwave pulse caused by air breakdown. A Bragg scattering experiment, using the plasma layers as a Bragg reflector is then performed. Both time domain and frequency domain measurements of wave scattering are conducted. The experiment results are found to agree very well with the theory. Moreover, the time domain measurement of wave scattering provides an unambiguous way for determining the temporal evolution of electron density during the first 100μs period. A Langmuir double probe is also used to determine the decay rate of electron density during a later time interval (1ms to 1.1 ms). The propagation of high power microwave pulses through the air is also studied experimentally. The mechanisms responsible for two different degree of tail erosion have been identified. The optimum amplitude of an 1.1μs pulse for maximum energy transfer through the air has been determined.

I. INTRODUCTION:

It is a well known fact that conventional line of sight radars are limited by their range of detection. This limitation is removed, however, by over-the-horizon (OTH) radars[1]. OTH radars use ionospheric plasma to reflect obliquely incident radar pulses back to the ground a distance away from the radar site. The range of detection is, in general, from 1000 to 4000 km which is far outside the range of line of sight (about 400km). Since the radar pulses are coming down from the ionosphere, moving targets can be detected, in principle, at any altitude. The extended range of detection of OTH radars can also be used to monitor ships and oceans from a land base. Moreover, OTH radar can also be used for air traffic control in areas where the simple line of sight radars can not reach. The above mentioned attractive applications of the OTH radar in turn generate a great deal of concern on how to improve the sensitivity of the OTH radar.

It is believed that the sensitivity of an OTH radar can be improved if the capability of the OTH radar can be extended with respect to three major factors. The first one regards the range of the radar. In order to avoid cluttering in the radar return, a large clearance region which is proportional to the height of the ionospheric reflector is required. The next concerns the resolution of the radar which depends strongly on the radar frequency. The last concern is on the stability of the ionosphere, which varies from day to night. This variation will affect the performance and reliability of the radar.

These concerns may be resolved if a reflector can be positioned at a much lower altitude which is able to reflect radar pulses of much high frequency. In addition, if the reflector is made artificially, its stability and location are controllable. Two schemes have been proposed. Both schemes use a high power RF breakdown approach for plasma generation[2-5]. The RF pulses used for air breakdown and plasma maintenance will be transmitted by ground based phased array antennas. In the first scheme, only a single focused RF beam will be employed to produce an ionization patch in the D region of the ionosphere. The RF beam is required to be focused because the altitude is well above the altitude of minimum breakdown threshold. Consequently, the cross section of the beam at the patch altitude will be too small in comparison with the Fresnel size, and a scanning process must be in cooperated in the operation of the RF beam in order to enlarge and tilt the ionization patch. The density of the patch is expected to be only slightly higher than that of the F-peak (i.e. $n_e \cong 10^6 cm^{-3}$). The schematic arrangement

The second scheme can, however, remedy these difficulties. Two crossed beams are proposed[5] to be used for plasma generation in their intersection region, at an altitude between 30 and 60 km[1,2]. The interference between the fields of the two beams enhances the peak field amplitude and, thus, reduces the required power level of each RF beam. This, in turn, helps to reduce the propagation loss in pulse energy before the two beams intersect. In fact, more energy will be delivered to the destination because the pulse tail erosion problem can be almost completely suppressed, especially when the intersection altitude is chosen to be near 50km (1 torr pressure)[6] where the breakdown threshold is minimum (so that the most effective ionization patch can be achieved). Such a low altitude can be used because the ionization patch will be tilted automatically to a large angle (the average of the propagation angles of the two beams). Moreover, the ionization patch consists of a set of parallel plasma layers which are the consequence of interference between the fields of two beams[6,7]. In the intersection region, field amplitude varies periodically in space in the direction perpendicular to the plane bisecting the two beams. Using Bragg reflection to replace conventional plasma cutoff reflection, the supplemental radar may be possible to operate at much high frequency. Using this scheme, the location of the ionization layers can also be fixed easily. A schematic of the scheme is shown in Figure 2.

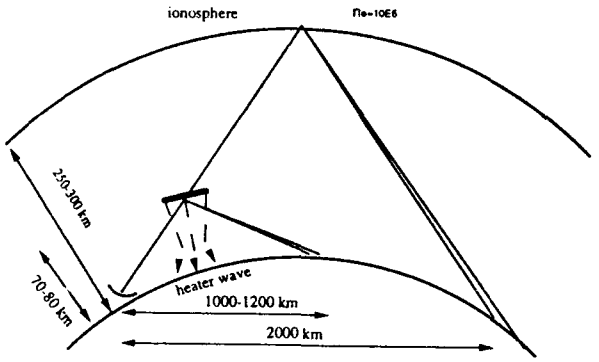

Fig. 1. OTH radar using artificial plasma patches as a mirror

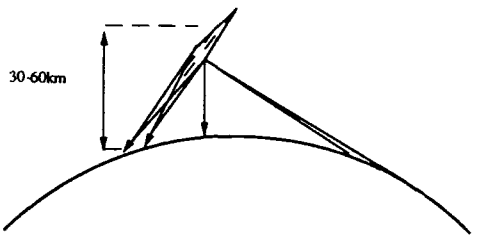

Fig. 2. Two crossed beams scheme

We have conducted a chamber experiment to examine the scientific feasibility of the second scheme. In order to achieve a meaningful simulation of the scheme, three major issues will be addressed by our chamber experiments. These include 1) the effectiveness of the plasma layers as a Bragg reflector, 2) the propagation of high power microwave pulse (HMP), and 3) the lifetime of the plasma.

The organization of this paper is as follows. The experimental set-up is described in Sec. II. The results of an experiment determining the characteristics of air breakdown by microwave pulses are also presented. The Bragg scattering experiment is reported in Sec III. Measurements in both time domain and frequency domain on scattering are performed and compared with the theory. In Sec. IV the propagation of high power microwave pulses through the chamber is studied. Two different tail erosion mechanisms are identified experimentally. The optimum pulse amplitude for maximum energy transfer through the air is also determined. Described in Sec.V is the measurement of Langmuir probe on the density and temperature of plasma electrons. These results together with those extracted from the Bragg Scattering measurement are used to determine the lifetime of plasma electrons. This work is summarized and discussed in Sec VI.

II. EXPERIMENTAL SET-UP AND AIR BREAKDOWN BY MICROWAVE PULSES

Experiments are conducted in a large chamber[6] made of 2 foot cube of Plexiglass and filled with dry air to a pressure corresponding to the simulated altitude. The microwave power is generated by a single magnetron tube (OKH1448) driven by a soft tube modulator. The magnetron delivers 1 megawatt peak output power at a center frequency of 3.27 GHz. The modulator uses a pulse forming network having a pulse width which can be varied from 1.1μs to 3.3μs with respective repetition rates from 60 to 20 Hz. Two microwave beams are fed into the cube, with parallel polarization direction, by two S-band microwave horns placed at right angles to the adjacent sides. The plasma layers are then generated in the central region of the chamber where the two beams intersect. Shown in Fig. 3 is a photo of the plasma layers which are manifested by the enhancement of airglow from the corresponding locations. A maximum of eight layers can be generated, thought only seven of them are shown in the photo. Shown in Fig. 4(a) is the typical envelope of a 1.1μs pulse used for plasma generation. Using a focusing lens to localize the enhanced airglow, its temporal evolution between the two consecutive pulses is then recorded on the oscilloscope through a photomultiplier tube. A typical result is shown in Fig. 4(b), which shows the growth and decay of the enhanced airglow. Breakdown of air[8] was detected either visually, as the first sign of a glow in the chamber, or as the distortion in the shape of the pulse received by the horn placed at the opposite side of the chamber. The dependence of the breakdown threshold field as a function of the pressure

Fig. 3. Plasma Layers Produced by crossed microwave beams

(a) (b)

Fig. 4. The optical measurement of the airglow from a plasma generated by two intersecting 1.1μs microwave pulse (a) Envelope of 1.1μs microwave pulses the horizontal axis is 200ns/division 4(b) growth and decay of the enhanced airglow

is then measured. The microwave field is measured by a microwave probe which has been calibrated by a known waveguide field. Shown in Fig. 5 are the Paschen breakdown curves for the cases of 1.1μs and 3.3μs pulses. Since a shorter pulse requires a larger ionization rate in order to generate the same amount of electrons, the threshold field is, therefore, accordingly increased. This tendency is clearly demonstrated in Fig. 5. It shows that the breakdown threshold field for 1.1μs pulse is always larger than that for a 3.3μs pulse. The results also show that in both cases, the breakdown threshold field decreases with a decrease in air pressure and reaches a minimum in the 2 to 1 torr region where $\omega \equiv \nu_c$; ω and ν_c are the microwave frequency and the electron-neutral collision frequency, respectively. With a further decrease in the pressure, the breakdown threshold field increases again. The increase of the threshold field happens also because the wave is in the pulse mode. The ionization frequency and collision frequency are proportional to the neutral density; lower pressure requires a larger field in order to maintain the ionization frequency.

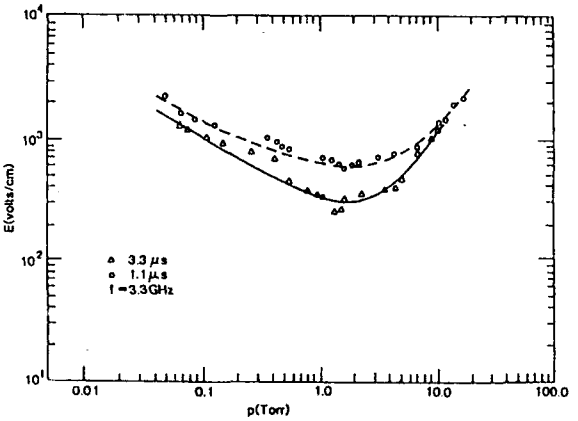

Fig. 5. Dependence of the air breakdown threshold field on the pressure for two pulse lengths breakdown curve for 1.1μs and 3.3μs pulses

The dependence of the breakdown threshold field on the pressure is also manifested by a similar dependence of the degree of attenuation in the tail portion of a single transmitted pulse through the chamber. The experiment is performed by reducing the chamber pressure consecutively from 8 torr to 50 m torr, while the incident pulse is fixed at constant amplitude. A series of snap shots demonstrating this behavior is presented in Fig. 6. In the high pressure region (≥ 8 torr), the breakdown threshold field is higher than that of the incident pulse, and therefore, very little ionization can occur; thus, the pulse can pass through the chamber almost without any distortion (Fig.6(a)).

However, as the pressure drops, the breakdown threshold also decreases before reaching the minimum, and hence, more ionization occurs and so does more distortion to the pulse (Fig. 6(b)). The distortion always starts from the tail portion of the pulse (i.e. tail erosion) because it takes finite time for the plasma to build up and thus, maximum absorption of pulse energy by the generated electrons always appears in the tail of the pulse. Consequently, the leading edge of the pulse is not affected. Between 2 to 1 torr, the pulse appears to suffer maximum tail erosion and hence only the very narrow leading edge of the pulse can pass through the chamber (Fig. 6(c)). The tail erosion becomes weak again for a further decrease in the pressure (Fig. 6(d)) and eventually vanishes (Fig. 6(e)) once the pressure becomes so low (≤ 0.05 torr) that the breakdown threshold power exceeds the peak power of the incident pulse.

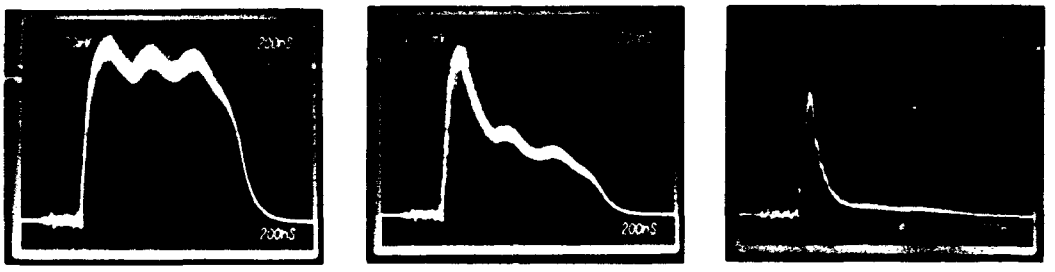

(a) p=8 torr (b) p=4 torr (c) p=1 torr

(d) p=0.45 torr (e) p=0.1 torr (f) p=0.05 torr

Fig. 6. Pulse propagating through chamber at different air pressure at different pressure

III. BRAGG SCATTERING

The plasma layers generated by the two crossed microwave pulses are used for the Bragg scattering study[6]. The spatial distribution of the plasma layers is first measured with a Langmuir double probe. This is done by using a microwave phase shifter to move the plasma layers across the probe. The peak density distribution for a spatial period is thus obtained and presented in Fig.7. The result shows that we have indeed produced very sharp plasma layers with very good spatial periodicity. A Bragg scattering experiment has then been conducted and described as follows.

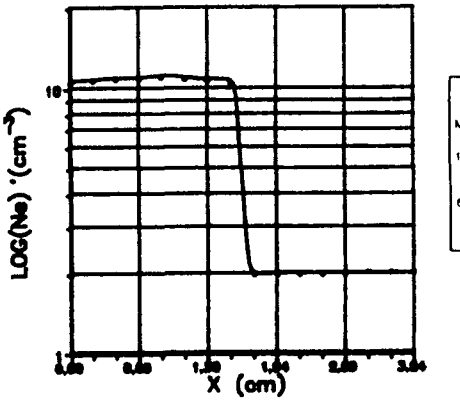

Fig. 7. Probe measurement of the plasma peak density distribution along the direction transverse to the plasma layers. Measurement is fromthe central point x=0 of one layer to the midpoint x=3.24 of the next layer

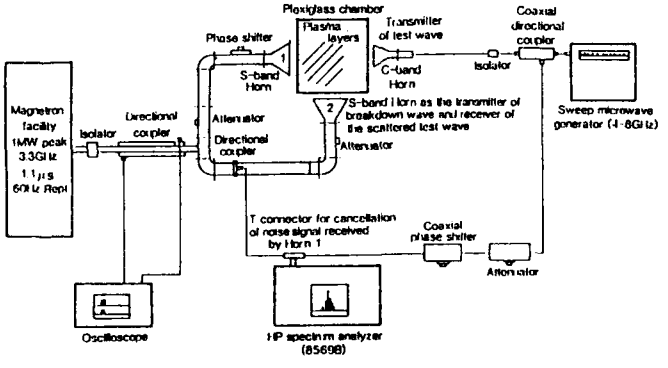

Fig. 8. Microwave Bragg scattering experiment setup

Presented in Fig. 8 is a block diagram of the experiment setup. In addition to the facility used for plasma generation (located to the left of the Plexiglass chamber), a sweep microwave generator (4-8 GHz) is used to generate a test wave which is incident into the chamber through a C-band horn. The incident angle of the test wave with respect to the normal of the plasma layers is 45 degrees. hence, the S-band horn #2 located at a right angle to the adjacent side can be used as the receiver of the Bragg scattering test wave. In order to separate the Bragg coherent reflection mechanism from the cutoff reflection mechanism, the test wave is swept in a frequency range much higher than the plasma cutoff frequency. Consequently, the test wave will be received by the S-band horn #1 even while the plasma is present. The amplitude of this undesired signal is reduced by using a directional coupler, nevertheless, it represents a large noise to the real scattering signal. To resolve this problem, a standard noise cancellation technique is used. The microwave components used for noise cancellation are shown in the diagram (Fig. 8). An HP spectrum analyzer (8569B) is used for recording the scattering signal. It is noted that the attenuation of the directional coupler is frequency dependent. Only test waves with frequencies leading to mare than 15 db attenuation of the directional coupler are used in the experiment. Consequently, the perturbations of the noise signal due to the presence of the plasma, which in principle is in the same intensity level as the scattering signal, is reduced by 15 or more db and will not affect the measurement of the Bragg scattering signal.

(a) (b)

Fig. 9. Spectrum analyzer CRT display. (a) No signal is received when the plasma is off.
(b) The spectrum of scattered signal detected when plasma layers are present.

Presented in Fig. 9 are the outputs of the spectrum analyzers for two cases. Fig. 9(a) shows that no signal is received when there is no plasma. However, an appreciable scattering signal is detected, as shown in Fig. 9(b) whenever the plasma layers are produced. The frequency of the test wave is 4.01 GHz, which is much higher than the cutoff frequency. A clear signature of Bragg scattering has been demonstrated. The temporal evolution of the scattering signal has also been measured. The result for a test wave with frequency 6.6 GHz is presented in Fig. 10(a). For comparison, one of the two microwave pulses (both are 1.1μs) used for plasma generation is shown in Fig. 10(b). As one can see, the scattering signal continues to persist for about 100μs after the breakdown pulses are turned off. This result indicates that the coherent scattering process can be very effective even when the plasma is well below (≈ 2 order of magnitude) the cutoff frequency of the test wave.

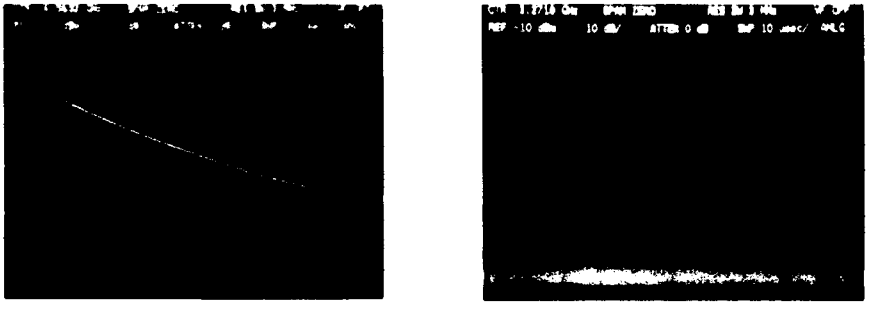

(a) (b)

Fig. 10. The time domain measurement of the scattered signal and the microwave pulse used for plasma generation. 10μs/division
(a) Growth and decay of the scattered signal over a 100μs time interval. (b) 1.1μs pulse envelope shown at the same time scale

The next question is how the experimental results compare with the theory. Considering a set of N parallel plasma slabs with thickness δ and separation d, and using the Bragg condition $2d\sin\theta = n\lambda_s$ where θ is the angle of Bragg scattering, λ_s is the wavelength of the scattered wave, and n is a positive integer, the scattering (reflection) coefficient S of wave intensity is derived analytically and expressed as

$$S = |E_r/E_i|^2 = (k_i^2\alpha/2)^2[\sin(n\pi\delta/d)/(n\pi/d)^2]^2[\sin N\theta_J/\sin\theta_J]^2 \qquad (1)$$

where E_t and E_r are the field amplitude of test wave and scattering wave, respectively, $\alpha=\omega_{pe}^2/\omega_t(\omega_t^2+\nu_e^2)^{1/2}$; k_t and ω_t are the wave number and frequency of test wave, and $\theta_t=(\omega_t-\omega_s)d\sin\theta/c$ and $\omega_s=2\pi c/\lambda_s$. This reflection coefficient is then plotted as a function of the test wave frequency in Fig. 11. By sweeping the test wave frequency, such a dependence is also determined experimentally in a relatively small frequency range (4.3 GHz to 7.8 GHz) and presented in Fig. 11 for comparison. The frequency dependencies of output intensity of the sweep generator and the antenna gain of the receiving horn (S-band horn#2) have been examined and taken into account in calibrating the intensity of the scattering signals. Though a maximum eight layers can be produced, only three of them have significant overlap along a line of sight. Therefore, only these layers can significantly contribute to the Bragg scattering process. Besides an uncalibrated absolute magnitude, the two functional dependencies are shown to agree with each other very well. It is noted that the separation d between the two adjacent plasma layers is related to the wavelength λ_0 of the microwave pulse and the angle ϕ between the propagation directions of the two intersecting pulses.with the relationship $d = \lambda_0/2 \sin(\phi/2)$ Using the Bragg condition $2d\sin\theta = n\lambda_s$, the optimum frequency for Bragg scattering is given by

$$f_s=nf_0\sin(\phi/2)/\sin\theta \qquad (2)$$

In the present experiment, $\phi = 90^\circ$, and thus $f_S=nf_0$. This indicates that the frequency of the test wave, which satisfies the Bragg condition for the current experimental arrangement, is equal to the frequency and its harmonics of the breakdown pulses. Consequently, the breakdown wave can not be filtered out and represent a very strong noise, which prevents any meaningful test of Bragg scattering at these frequencies, and in fact, also in the neighborhood frequency regions. Although the optimum frequency region for Bragg scattering is not examined, nevertheless the consistency between prediction and experimental results may lead us to conclude, based on the maximum theoretical reflection coefficient, that plasma layers can indeed be an effective Bragg reflector, especially if more layers can be produced for scattering purposes.

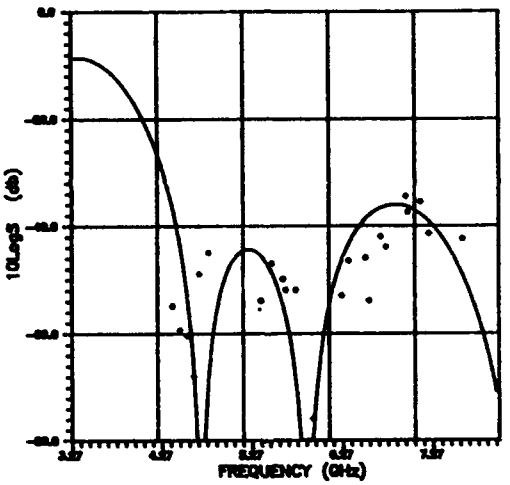

Fig. 11. The dependence of the reflectivity S of plasma layers on wave frequency. Experimental and theoretical results. The 0db on the vertical axis is an arbitrary reference

IV. PROPAGATION OF HIGH POWER MICROWAVE PULSES THROUGH THE CHAMBER

The propagation of high power microwave pulses through the atmosphere has been a subject with considerable scientific interest.[3-8] This is because air breakdown produces ionization phenomena that can radically modify wave propagation. Ionization gives rise to a space-time dependent plasma which attenuates the tail of the pulse but hardly affects the leading edge because of the finite time for the plasma to build up. A mechanism which is called " tail erosion" plays the primary role in limiting transmission of pulse.[9-11,14] Moreover, the nonlinear and non-local effects brought about by the space-time dependent plasma also play important roles in determining the propagation characteristic of the pulses.[13] Therefore, any meaningful theoretical effort requires a self-consistent description of the propagation process. Consequently, an experimental effort could be more relevant and useful.

Basically, there are two fundamental issues to be addressed. One concerns the optimum pulse characteristic for maximum energy transfer through the atmosphere by the pulse. The second concern is maximizing the ionizations in the plasma trail following the pulse. In general, these two concerns are interrelated and must be considered together. This is because in order to minimize the energy loss in the pulse before reaching the destination, one has to prevent the occurrence of excessive ionization in the background air. Otherwise, the overdense plasma can cutoff the propagation of the remaining part of the pulse and cause the tail of the pulse to be eroded via the reflection process. This process is believed to be far more severe in causing tail erosion than the normal process attributed to ionization and heating. Once this process occurs, the remaining pulse will become too narrow to ionize dense enough plasma.

The purpose of our experimental effort is to understand the fundamental behavior of tail erosion and address the question of how energy loss depends on basic parameters such as pulse intensity and background pressure. The experimental data can then be incorporated for the development of an useful theoretical model for a self-consistent derivation of pulse propagation.

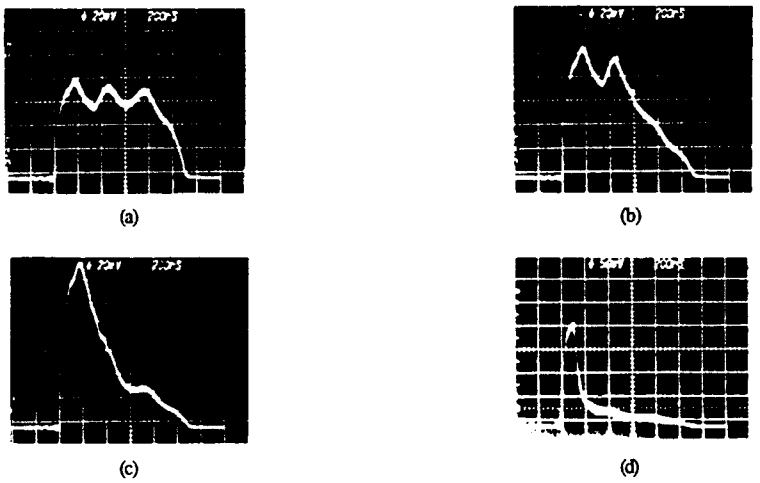

Fig. 12. Tail erosion of microwave pulses of four consecutively increasing amplitudes A_0 - A_3 after propagating through the chamber with 1Torr background pressure (a) Amplitude A_0 below the breakdown threshold and no erosion. (b) $A_1 = 1.5A_0$. (c) $A_2 = 2A_0$. (d) $A_3 = 3A_0$

Tail erosion phenomenon is demonstrated by the snap shots presented in Figure 12, where 1.1μs pulses, with four consecutively increasing amplitude, are transmitted into the chamber of 1 torr pressure from one side and received from the opposite side. The first pulse has amplitude below the breakdown threshold, and hence, nothing is expected to happen. Consequently, the received pulse shape (Fig.12(a)) is undistorted from that of transmitted pulse. Once the amplitude exceeds the breakdown threshold, more tail erosion occurred to the larger amplitude pulses, as is observed by the subsequent three snap shots (Figs.12(b)-12(d)). This is because the increase of the ionization rate with field allows more electrons, which attenuate the pulse, to build up. Now let's focus on the last two pictures (Figs.12(c) and 12(d)). Pulses have been eroded strongly in both cases. However, a clear distinction between the two cases is noticed. In one case corresponding to the third picture (Fig.12(c)), the erosion to the tail of the pulse is not complete. In other words, the received pulse width extends to the original width. In the other case (Fig.12(d)), a large portion of the pulse is more or less eroded completely during the finite propagation period. Obviously it is a different mechanism responsible for the second case. The ionization frequency becomes so large in the second case that the electron density exceeds the cutoff density of the wave before the whole pulse passes through. The overdense plasma screen reflects the remaining portion of the pulse and causes even more severe tail erosion. In summary, two mechanisms responsible for the tail erosion are identified. One is due to attenuation by the self-generated underdense plasma. The other one is caused through reflection by the self-generated overdense plasma screen. These two processes are also verified by the reflected power level measured for each case. As shown in Figure 13, the snap shots (Figs.13(b) and 13(d)) presented on the RHS of the Figure are the reflected pulse shape corresponding to each received pulse on the left (Figs.13(a) and 13(c)). As shown by the last set of pictures (Figs.13(c) and 13(d)), strong reflection and complete erosion are observed consistently.

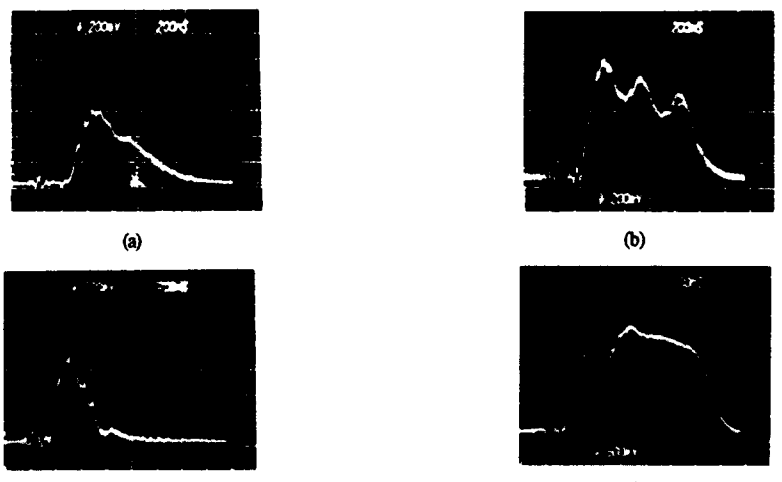

Fig. 13. Received pulses and corresponding reflected pulses. (a) Envelope of received pulse. (b) Reflected pulse corresponding to case (a). (c) received pulse with larger incident amplitude than that of case (a). (d) Reflected pulse corresponding to case (c).

In order to avoid cut off reflection, the power of the pulse should be lower than a critical power Pr which is defined as the minimum required power for generating an overdense plasma screen. When an overdense plasma screen is formed the shape of the reflected pulse changes drastically and can be monitored easily. Thus, the critical power Pr can be determined. This critical power varies in general with the pressure . Measurements is made to determine its functional dependency on the pressure as shown in Figure 14, where P=Pr/Pc is the critical power normalized to the breakdown threshold power Pc whose dependencies on the pressure and pulse width are shown in Fig.5. Due to the limitation on the power of our microwave facility, only region of 0.2 to 10 torr for the critical power is examined. Nevertheless, this is the pressure region of main concern because air breakdown has its lowest threshold.

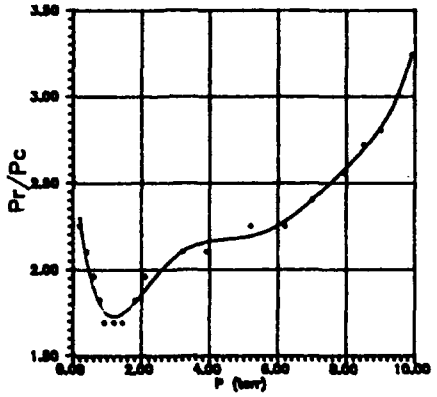

Fig. 14. The dependence of the normalized critical power $P=P_r/P_c$ on pressure for 1.1μs pulse.

Our study indicates that an increase of pulse amplitude may not help to increase the energy transfer by the pulse. This is because two tail erosion mechanisms are at play to degrade the energy transfer. A demonstration is presented in Figure 15, where the growth and decay of airglow enhanced by electrons through air breakdown by 3.3μs pulse are recorded for two different power levels. In Figure 15(a) the power level is below the critical power and the airglow grows for the entire 3.3μs period of the initial pulse width. As power is increased beyond the critical value, the initial growth of the airglow becomes faster as shown in Figure 15(b). However, it is also shown in Figure 15(b) that the airglow saturates at about the same level as that of Figure 15(a). Moreover, the airglow already starts to decay even before the 3.3μs period. In other words, cutoff reflection happening in the second case limits the energy transfer by the pulse. The additional energy added to the pulse is wasted by reflection. The way to solve the problem is either to lower the amplitude of the pulse or to narrow the pulse width so that the propagation loss can be minimized.

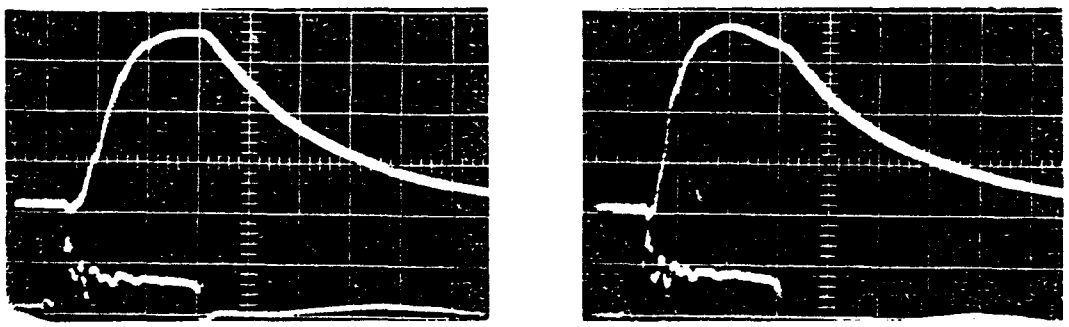

(a) (b)

Fig. 15. The growth decay of enhanced airglow (upper trace). Pulses of 3.3μs duration and at two different levels P_1 for (a) and P_2 for (b) are used for causing air breakdown, where $P_2/P_1 = 1.32$. The lower trace of each photo represents the time dependence of the microwave pulse. The horizontal scales are 1μs/div.

V. LIFETIME OF ELECTRONS

For practical purpose, the lifetime of plasma generated by microwave pulses is interested. Since in the application, e.g. use of plasma as a reflector of OTH radar, One would require that the plasma is sustained at or above certain electron density level (e.g. $10^7 cm^{-3}$ one order of magnitude higher than that of the F peak) for long enough time (e.g. about 1 sec of the operation time of the radar), it could be done by using repetitive pulses. However, if plasma decays very fast, one would have to increase the duty cycle of microwave facility (i.e. the repetition rate of the pulse). It implies that more power is needed in the operation. This is then translated as that more expensive microwave facility will be required and more running cost will be resulted. On the other hand, if plasma is shown to have desired long lifetime, the current technology is already ready for required specifications. The design of the system becomes straightforward and more important, the whole system can be justified to be economically feasible and competitive.

In general, there are three processes work together to cause the decay of the plasma. They are electron diffusion, electron-ion recombination, and attachment of electrons to the neutral molecules. For the case of 1 torr background pressure, electron-neutral collision frequency is about GHz. The free electron diffusion coefficient D is estimated to be about $3x10^4$ cm^2/sec. Thus, the diffusion time for free electron to walk randomly from the center of the chamber to the side walls is calculated to be about 20 ms. If the ambipolar effect is taken into account, the diffusion time becomes even larger and is in the order of seconds. Therefore, we simply ignore the diffusion effect on the electron decay rate in the present study. Since the carrier frequency of microwave pulses is 3.27 GHz, the peak electron density ionized by the microwave pulses is in the order of 10^{11} cm^{-3}. Thus, the electron-ion recombination rate is always smaller than the electron attachment rate whose maximum value at 1 torr pressure of air is about $1.4x10^5$ cm^{-1}. We therefore expect that the initial decay rate (i.e. the maximum decay rate) of the electrons is determined by the electron attachment rate and is somewhat bounded by this value $1.4x10^5$ sec^{-1}.

As given by (1), Bragg scattering coefficient S of wave intensity is directly proportional to n_e^2. Hence, the Bragg scattering experiment with the produced plasma layers described in sec.III also provides a way for a nondestructive measurement on the temporal evolution of plasma electron density. Using the result, shown in Fig. 10(a), of the temporal evolution of the scattering signal from a test wave, the electron decay rate after the breakdown pulses have passed through (i.e. the initial decay rate) is evaluated to be $6x10^4$ sec^{-1}, which is consistent the dissociative attachment rate. It also shows that the electron density after 70μs is reduced by a factor of about 30. Similarly, the electron decay rate is also reduced over a factor of 10 from the initial decay rate. In this density level ($\approx 3x10^9 cm^{-3}$) the decay rate is consistent with the recombination loss rate. This is realized by the fact that when enough negative molecule ions are produced through the electron attachment process, the detachment rate for electron regeneration is increased and eventually balances out the electron attachment loss rate. Thus, the dominant electron loss mechanism is shifted to the recombination process. On the other hand, the attachment process also plays the role to reduce the recombination and diffusion losses of electrons. Through the attachment process, the excess of free electrons is first stored by attaching themselves to the low mobility neutral molecules and then released to be the source of free electrons of the system whenever there is a need for the balance among all the process involved. When such a balance is reached (e.g. 70μs point of Fig. 10(a), free electron density will only decay at a relatively slow rate determined by the recombination process and the ambipolar diffusion process.

With the available power ($\approx$10mw) of sweep microwave generator and the detecting facility (HP spectrum analyzer 8569B), the Bragg scattering measurement is no longer sensitive to the electron density at the level after 100μs decay from its peak (i.e. Fig 10(a)). The evolution of electron density at later time is then determined by a Langmuir double probe. The main purpose of Langmuir probe measurement is to confirm that the decay of electron density after the balance of process is reached is indeed caused mainly by the recombination process. As an additional payoff, the probe measurement can also provide the information on electron temperature. The difficulty with Langmuir probe measurement lies on the presence of negatively charged molecules so that the ion density is not quite the same as the electron density. The presence of negatively charged molecules also complicates the relationships among the electron density, electron temperature, and ion density etc. inside a sheath. For instance, the sheath potential changes its sign when the density of negatively charged molecules becomes much larger than that of free electrons. It can be monitored experimentally by the direction of current flow through a grounded single probe. We, therefore, report only the results in the time interval in which the percentage of negatively charged molecules is effectively low. Shown in Fig.16 is the Langmuir double probe measurement of temporal evolution of electron temperature $T_e(t)$ during the first 18μs right after the passing through of the microwave pulses. It shows that electron temperature is heated by the microwave pulses to about 1eV and decreases quickly after the microwave is turned off. The decay rate is about $10^5 sec^{-1}$ which is consistent with the electron energy loss rate via electron-neutral collision. The correspondi g evolution of electron density can be drawn from the result of Fig. 10(a).

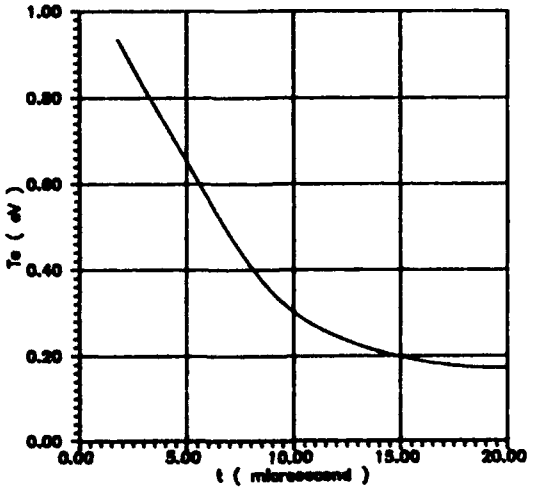

Fig. 16. Langmuir double probe measurement of temporal evolution of electron temperature $T_e(t)$

We next report the measurement for 100μs period starting at 1ms after turning off the microwave. The V-I characteristics of the Langmuir double probe at four different times are presented in Fig. 17. These Curves having a same slope at I_p=0 indicate that all the species of the gas have already reached thermal equilibrium and have a temperature ≈300°k. However, these curves saturate at different current levels. It indicates that ion density still varies with time. Based on the saturation levels of these curves, the evolution of ion density with time is determined. In this time interval (1ms,1.1ms) electron density can be assumed to be in the same order of magnitude as the ion density. The evolution of electron density is thus determined and plotted in Fig. 18. The decay rate of 500 sec^{-1} is indeed consistent with the recombination rate at this density level.

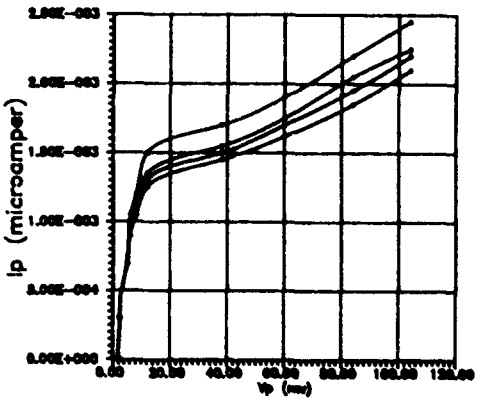

Fig. 17. The V-I characteristics of the Langmuir double probe at four different times

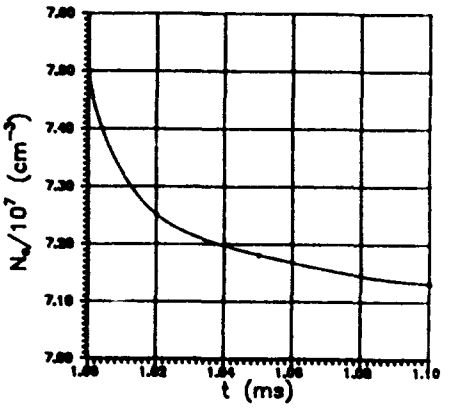

Fig. 18. The evolution of electron density in time interval (1ms,1.1ms)

We have shown that in the density region of interest the decay rate of electron density is governed by the electron-ion recombination rate. Based on this decay rate, repetitive pulses with a repetition rate about 250 sec^{-1} will suffice for maintaining the electron density to a level ($\approx 10^7 cm^{-3}$), which is high enough for the OTH radar applications. Moreover, the pulses used for maintaining the plasma can be much shorter than the first pair of triggering pulses which have to start the ionization from relatively low background electron density. Therefore, the required microwave power and energy for plasma generation and its sustainment can be shown to be within the state of the art of current technology.

VI. SUMMARY AND DISCUSSION

Plasma layers generated by two intersecting microwave pulses are used for the study of Bragg scattering. The experiment is conducted in a large chamber with a microwave absorber so that the microwave reflection from the wall can be minimized. Hence, the experiment can be considered to be a laboratory simulation of conceptualized plasma layers generated by high power radio waves in the upper atmosphere, as investigated theoretically by Gurevich.

We first determine the characteristic of air breakdown by powerful microwave pulse. This is mainly because the plasma generated near the wall adjacent to the microwave horn causes erosion of the tail of the incident pulse and the pulse becomes too short, by the time it reaches the central region of the chamber, to cause appreciable ionization. However, this problem is easily overcome when the scheme of two intersecting pulses is used for plasma generation. In this approach, each pulse has its field amplitude below the breakdown threshold to avoid the tail erosion. However, the fields in the intersecting region can add up and exceed the breakdown threshold. This scheme is most effective when the two pulses have the same polarization and are coherent. In this case, the wave fields form a standing wave pattern in the intersecting region in the direction perpendicular to the bisecting line of the angle ϕ between the intersecting pulses. Thus, parallel plasma layers with a separation $d=\lambda_0/2\sin(\phi/2)$ can be generated. This result is shown in Fig. 1.

Since there are no electrodes involved in the current experiment of air breakdown, we can determine the breakdown threshold field as a function of the air pressure within the accuracy of microwave probe measurement. Two Paschen breakdown curves for the cases of 1.1 and 3.3μs pulses are determined as shown in Fig. 5. The appearance of a Pachen minimum can be explained as the result of breakdown by a short pulse which is equivalent to a dc discharge with short separation between electrodes (i.e. short electron transit time). The result that the breakdown threshold by a longer pulse (3.3μs) is lower than that by shorter pulse (1.1μs) agrees with the explanation. The characteristic of the curves is also confirmed phenomenologically by the various degrees of tail erosion of the same pulse passing through the chamber at different pressure, as shown in Fig. 6.

An optical probe has been used to monitor the growth and decay of airglow enhanced by microwave generated electrons. Two processes are, in general, responsible for the airglow. One is through the electron-ion recombination and the other one is through impact

excitation of natural gas. Since only weakly ionized plasma is generated, the second process is believed to be dominant. However, the second process requires that the electron energy exceed 2eV. Therefore, the decay rate of airglow intensity shown in Fig. 4(b) accounts for not only the decay of the electron density caused by the dissociative attachment loss but also for the decay of electron temperature caused by energy loss to the neutrals and the loss of fast electrons.

We then conducted the Bragg scattering experiment with the produced plasma layers. Both temporal evolution of the scattering signal from a test wave and the spectral dependence of the scattering coefficient have been examined. Good agreement between theoretical and experimental results on the spectral dependence of the scattering coefficient has been achieved (Fig.11). It should be noted that, due to the dimension of the chamber and microwave beams, only three plasma layers have significant overlap along a central line of sight used as the incident path of the test wave for Bragg scattering. Nevertheless, a remarkable effectiveness of Bragg scattering has been demonstrated by the chamber experiment. It is further realized that more layers and much larger cross sectional area for each layer will be produced in the actual installation. One would expect that much more plasma layers can be incorporated for Bragg scattering. Since the scattering coefficient is proportional to the square of the number of layers at play, effective Bragg scattering can still be achieved at even much lower plasma density ($\approx 10^7 cm^{-3}$ for practical application) than that of current experiment ($\approx 10^9 cm^{-3}$), where the radar frequency is also more than one order of magnitude lower than that of the test wave used in the current experiment.

An experiment investigating the propagation of high power microwave pulses through the air is also performed. We have identified two mechanisms which are responsible for two different degree of tail erosion. One is attributed to absorption by the self-generated underdense plasma. The other one is caused by reflection by the self-generated overdense plasma screen. Our study indicates that an increase of pulse amplitude may not help to increase the energy transfer by the pulse. This is because the two identified tail erosion mechanism are at play to degrade the energy transfer. A demonstration is presented in Figure 15, where the growth and decay of airglow enhanced by electrons through air breakdown by 3.3μs pulse are recorded for two different power levels. In Figure 15(a) the power level is below the critical power and the airglow grows for the entire 3.3μs period of the initial pulse width. As power is increased beyond the critical value, the initial growth of the airglow becomes faster as shown in Figure 15(b). However, it is also shown in Figure 15(b) that the airglow saturates at about the same level as that of Figure 15(a). Moreover, the airglow already starts to decay even before the 3.3μs period. In other words, cutoff reflection happening in the second case limits the energy transfer by the pulse. The additional energy added to the pulse is wasted by reflection. The way to solve the problem is either to lower the amplitude of the pulse or to narrow the pulse width so that the propagation loss can be minimized. The optimum pulse amplitude for maximum energy transfer through the air has been determined for 1.1μs pulse used in the present experiment. Since the effect of pressure gradient and large propagation distance can not be incorporated in chamber experiment, the determination of optimum parameters of the pulses for achieving the most effective plasma generation is deferred until a practical theoretical model developed under the guide of present study is established.

A practical issue concerning the applicability of present study to the OTH radar is the lifetime of plasma electrons generated by the microwave pulses. The theoretical result (1) shows that the scattering coefficient is proportional to the square of the electron density and insensitive to the electron temperature. Therefore, the electron decay rate after the breakdown pulses have passed through can be evaluated from Fig.10(a). It shows that the initial decay rate is about 6×10^4 sec^{-1} which is consistent with the dissociative attachment rate. It also shows that the electron density after 70 μs is reduced by a factor of about 30. Similarly, the electron decay rate is also reduced over a factor of 10 from the initial decay rate. In this region the decay rate is consistent with the recombination loss rate. This is realized by the fact when enough negative molecule ions are produced through the electron attachment process, the detachment rate for electron regeneration is increased and eventually balances out the electron attachment loss rate. Thus the dominant electron loss mechanism is shifted to the recombination process. Using Bragg scattering, the evolution of electron density can be measured only for 100μs. In order to be sure that the loss of electrons is indeed caused mainly by the recombination process which has acceptable low rate, a Langmuir double probe is used to measure the evolution of electron density at much later time (i.e. 1ms to 1.1ms). The result of probe measurement confirms the conclusion of Bragg scattering measurement.

Based on the results of our chamber experiments, it seems to us that the implementation of a Bragg reflector in the upper atmosphere (≈50km) by two intersecting microwave pulses transmitting from ground for potential OTH radar applications is technically feasible.

ACKNOWLEDGEMENT

This work is being supported by the Air Force Geophysical Laboratory through NASA Grant No. NAG 5-1051 and by the Air Force Office of Scientific Research Grant No. AFOSR-85-0316. Useful discussion with Dr. M.C. Lee is appreciated.

REFERENCES

1.J. M. Headrick, M. I. Skolnik, Proceedings of The IEEE Vol. 62 No. 6 June 1974

2. A. V. Gurevich, Geomag. Aeronom 12, 631 (1972).

3. A. V. Gurevich, Geomag. Aeronom 19, 428 (1979).

4. N. D. Borisov, and A. V. Gurevich, Geomag. Aeronom 20, 841 (1980)

5. A. V. Gurevich, Sov. Phys. Usp. 23, 862 (1981).

6. S.P. Kuo and Y.S.Zhang, Phys. Fluids B, 2(3), 667-673, 1990

7. A. L. Vikharev, V. B. Gil'denburg, O. A. Ivanov, and A. N. Stepanov, Sov. J. Plasma Phys. 10, 96 (19840; A. L. Vikharev, O.A. Ivanov, and A. N. Stepanov, Sov. J. Plasma Phs., 10, 460 (1985).

8. A. D. MacDonald, D. U. Gaskell, and H. N. Gitterman, Phys. Rev., 5, 1841 (1963)

9. W. M. Bollen, C. L.Yee, A. W. Ali, M. J. Nagurney, and M. E. Read, J. Appl. Phys. 54, 101 (1983); C. L. Yee, A. W. Ali, and W. M. Bollen, J. Appl. Phys., 54, 1278 (1983).

10. J. H. Yee, R. A. Alvarez, D. J. Mayhall, N. K. Madsen, and H. S. Cabayan, J. Radiation Effects Res. and Eng., 3, 152 (1984).

11. B. Goldstein and C. Longmire, J. Radiation Effects Res. and Eng., 3, 1626 (1984).

12. Wee Woo and J. S. DeGroot, Phys. Fluids, 27, 475 (1984).

13. J. H. Yee, R. A. Alverez, D. J. Mayhall, D. P. Byrne, and J. DeGroot, Phys. Fluids, 29, 1238 (1986).

14. S. P. Kuo Y. S. Zhang, and P. Kossey, J. Applied Phys., 67(6), 2762-2766, 1990

DISCUSSION

L. DUNCAN, US

I don't quite understand your equating of tail erosion with formation of a critical density layer. After forming an artificial reflecting layer, why does the experiment just not assume a geometry similar to the one discussed in the preceding paper? In this case the interference pattern would clearly be very dynamic, but this would not be equivalent to traditional descriptions of tail erosion.

AUTHOR'S REPLY

In our case, when cutoff layer is formed, the reflected pulse has different characteristics from that by an inserted conducting plane discussed in the preceding paper. The differences are
1. Plasma cutoff layer is not equivalent to a conductor; in the layer, the electric field is maximum instead of zero.
2. The reflected pulse has shorter pulse length than the incident pulse because the leading part of the pulse can always penetrate through the layer.
3. The cutoff layer has a size equal or smaller than the pulse's cross section. Therefore, the edge effect can significantly deteriorate the shape of the reflected pulse.
4. Experimental evidence: when cutoff layer is formed (as indicated by the anomalous reflection), the breakdown induced plasma loses the expected interference pattern.